

# COMPARISON OF MIMO RELAYING DEPLOYMENT STRATEGIES IN A MANHATTAN GRID SCENARIO

*Martin Fuchs, Christian Kaes, Ulrike Korger, and Martin Haardt*

Ilmenau University of Technology, Communications Research Laboratory  
P.O. Box 10 05 65, 98684 Ilmenau, Germany, Phone +49 (3677) 69 2613  
{martin.fuchs, christian.kaes, ulrike.korger, martin.haardt}@tu-ilmenau.de

## ABSTRACT

A methodology for comparing MIMO relaying deployment strategies is proposed and a number of strategies are compared in a Manhattan grid scenario. The focus is on the deployments rather than on the type of MIMO technique in use. Therefore, the system behavior is modeled based on the maximum achievable sum rate under a sum power constraint (also known as Dirty Paper Code bound) while taking into account a buffer model at the relays.

## 1. INTRODUCTION

The aim of this investigation is to compare the downlink capacity performance and costs of different MIMO decode and forward relaying deployment strategies including different relay node (RN) and base station (BS) positions, number of antennas, and transmit powers in a Manhattan grid scenario. The channel is simulated with the help of the IST-WINNER II channel model [1] and simulation assumptions are kept close to the working assumptions of that project. To be independent of the choice of MIMO space-time processing technique, the study proposes a methodology based on the maximum achievable sum rate under a sum power constraint when channel knowledge is available at the transmitter (also known as Dirty Paper Code bound). To that extend, the chosen assessment criterion is capacity improvement (which is also the goal in WINNER, see for example [2]) as opposed to a possible coverage extension. A simulation study on similar issues with amplify and forward RNs can be found in [3], however based on specific MIMO techniques and without exploitation of channel state information at the transmitter.

Only recently a growing research interest exists in theoretical capacity bounds for MIMO relay enhanced systems. It would have been an option to base the present study on such theoretical results rather than construct an approach around a single base station capacity limit. However, to our best knowledge the available work is not applicable to the system

of interest and does not easily apply to a measurement based channel model. For example, the results in [4, 5] are valid for a single user only and rely on the key assumption that the RNs are operating in full duplex mode and have two sets of antennas, one for transmission and one for reception, which is not the case in the WINNER system. These works present upper and lower capacity bounds for the Gaussian and Rayleigh channel, with more tight lower bounds in [5]. General capacity scaling laws for half duplex relays are given in [6], however again for a single user in a system with an asymptotically high number of relays.

Section 2 describes the deployments considered here and how their relative costs are assessed. In Section 3, the system model and the proposed comparison method is described together with its advantages and limitations. Basic system parameters can be found in Section 4 where the simulation results are discussed.

## 2. DEPLOYMENTS UNDER INVESTIGATION

In the following, the deployment scenarios under investigation are described. The simulated sections of the deployment patterns were chosen to minimize the irregularities caused by cutting the grid while maintaining a feasible simulation time. This results in slightly different segment sizes. To be independent of the size of the simulation grid, the deployment costs are based on BS and RN densities per square meter  $d_{BS}$  and  $d_{RN}$  and are given as the ratio  $d_{BS}/d_{RN}$ . Assuming that a relay is cheaper than a BS, a higher cost ratio indicates higher total costs. This simple ratio has the drawback that a scenario without RNs would yield infinite costs. Should one want to investigate this case, a coefficient such as  $\frac{d_{RN}+d_{BS}}{d_{BS}}$  could be an option since it is both normalized, yet still strictly monotonically increasing in both variables. A comparison to the case without relays was not attempted here, since already [2] as well as [7] conclude from such a comparison that relay enhanced cells should be a key enabler of 4G wireless networks.

The number of TX antennas is not included in the cost figure in this study. Instead, it simply yields a different performance, whose implication is discussed in the conclusions. Two different numbers of antennas at the TX have been simulated, yielding also a different relative performance of the deployments. This paper is limited to uniform linear arrays

---

Part of this work has been performed in the framework of the IST project IST-4-027756 WINNER II, which is partly funded by the European Union. The authors would like to acknowledge the contributions of their colleagues in WINNER II, although the views expressed are those of the authors and do not necessarily represent the project. The authors also gratefully acknowledge the support of the German Research Foundation (Deutsche Forschungsgemeinschaft, DFG) under contract no. HA 2239/1-2.

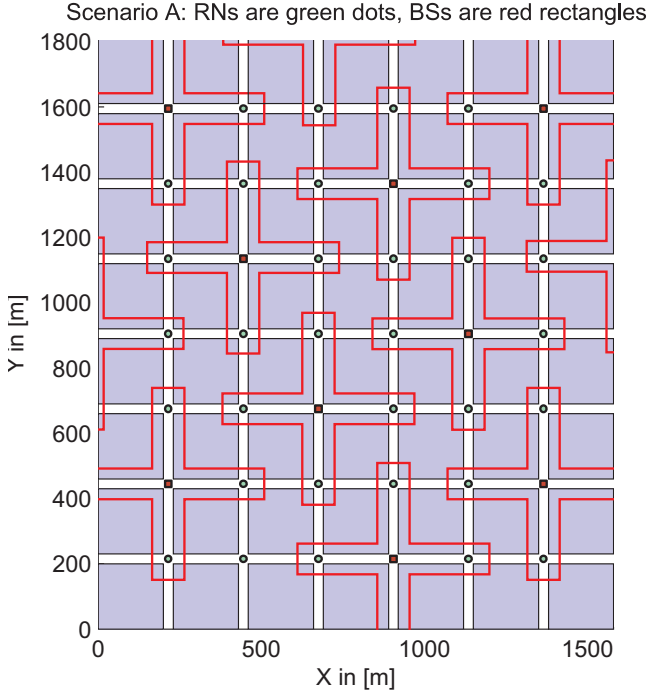


**Fig. 1.** Simulated section of deployment type 4D: Each transmitter mounts 4 ULAs facing in the street directions, arranged in a rectangle.

(ULAs), since this is the antenna geometry currently supported in the publicly available reference implementation of the IST-WINNER II channel model. Schematics of the deployments can be found in Figures 1-3.

**Deployment type 4D** is based on a 'plus' shape consisting of one BS and four relays as in [2]. In this scenario, the transmitters mount 4 ULAs pointing in the street directions, arranged in a rectangle. A grid of size  $7 \times 8$  building blocks was simulated (see Fig. 1). The variations considered can be distinguished by their label as follows: For example,  $4D8 P_{RN} = P_{BS}/5$  means that each BS and RN has a total of 8 transmit antennas (or 2 elements per ULA) and that RNs transmit with 1/5 of the BS power (default value given in [8]). We consider also  $4D8 P_{RN} = P_{BS}/3$ ,  $4D8 P_{RN} = 2P_{BS}/3$  as well as  $4D4 P_{RN} = P_{BS}/5$ ,  $4D4 P_{RN} = P_{BS}/3$  and  $4D4 P_{RN} = 2P_{BS}/3$ . The estimated cost coefficient of this deployment is 1.28.

**Deployment type 2D** is a diagonal deployment with BSs and RNs in the streets rather than on the intersections, similar to the basic deployment in [8]. The transmitters have 2 back-to-back ULAs facing in the street directions. A grid of size  $6 \times 6$  building blocks was simulated (see Fig. 2). Again we consider the variations  $2D8 P_{RN} = P_{BS}/5$ ,  $2D8 P_{RN} = P_{BS}/3$ ,  $2D8 P_{RN} = 2P_{BS}/3$ , and the respective cases with a total of 4 instead of 8 antennas. The estimated cost coefficient of this deployment is 1.5.

**Deployment type 1D** is a diagonal deployment much like the basic deployment proposed in [8], which is based on a 3G proposal. The transmitters have a single ULA facing towards 3 o'clock. A grid of size  $5 \times 6$  building blocks was simulated

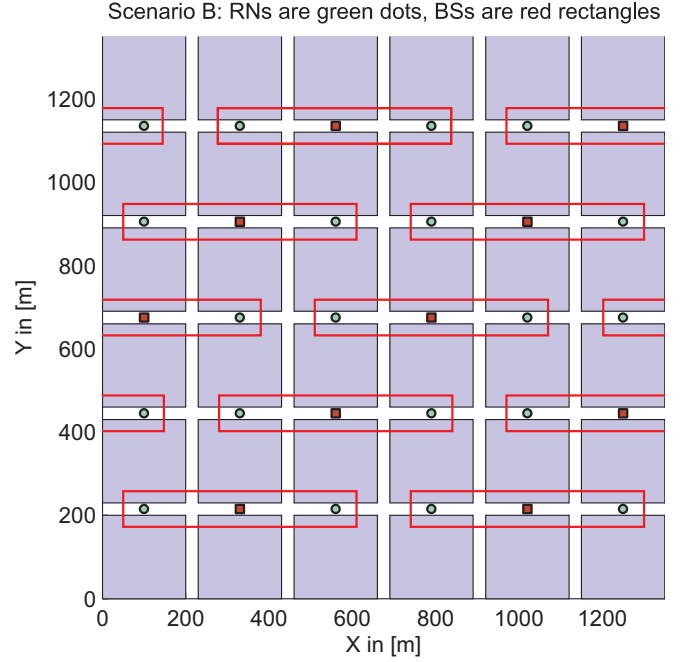


**Fig. 2.** Simulated section of deployment type 2D: Each transmitter mounts 2 back-to-back ULAs facing in the street directions

(see Fig. 3). As a result, only one RN per BS can be served due to the directivity of the antennas. Again we consider the variations  $1D8 P_{RN} = P_{BS}/5$ ,  $1D8 P_{RN} = P_{BS}/3$ ,  $1D8 P_{RN} = 2P_{BS}/3$ , and the respective cases with a total of 4 instead of 8 antennas. The estimated cost coefficient of this deployment is 1.92.

### 3. SIMULATION METHODOLOGY

Performance figures are obtained per square meter to account for the slightly different sizes of the deployment sections. For the same reason, the total number of users in the system is not fixed, but is obtained from a user terminal (UT) density per square meter which was set to  $10^{-5}/m^2$ .

The basic design of the relay enhanced system is close to that of [2]: Relays do not transmit and receive at the same time, resulting in the TDD frame structure given in the reference with a maximum of two hops foreseen. Frequency reuse is set to one as given in the baseline system description [8], i.e., no separation between the transmitting sites is considered. The latter two aspects should be treated in further studies.

As mentioned in the introduction, the focus is on the deployments rather than on specific MIMO technologies. For the reasons given in the introduction, the method proposed in the following is based on the rates achievable in the case of a single BS under a sum rate maximization with sum power constraint (the so-called Dirty Paper Code bound rates). To compute those rates and the corresponding transmit covariance matrices we decided to use the iterative uplink algorithm of [9] (whereas later uplink-downlink duality is applied, see

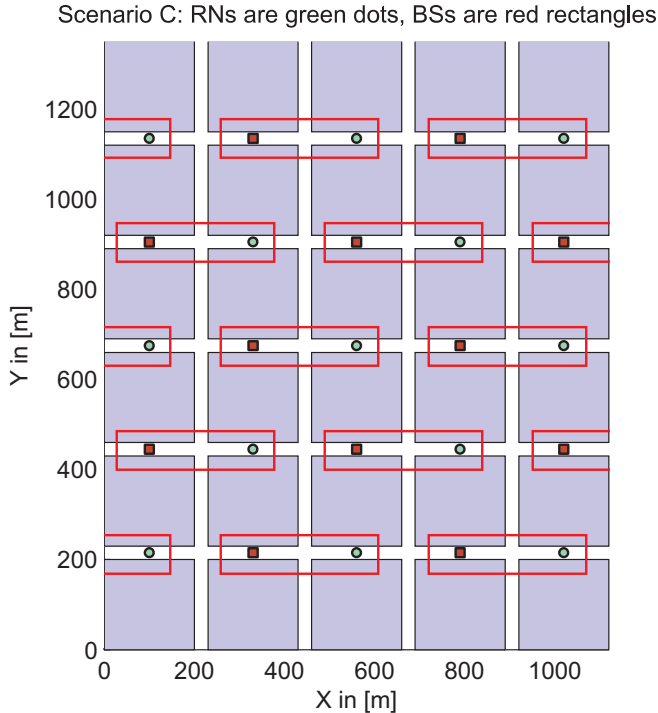


**Fig. 3.** Simulated section of deployment type 1D: The transmitters have a single ULA facing towards 3 o'clock.

the simulation steps described below). This algorithm was chosen amongst others because it has only one parameter, namely the desired convergence accuracy of the sum rate, and because it was observed to be the most numerically stable when the absolute values of the channel gains are very small as is the case when path loss and shadowing is included in the channel matrix. As a consequence of this approach, only one subcarrier can be considered in the simulations and the possibility of using OFDMA (which is given in the basic design of [2]) cannot be investigated. This is due to the fact that in the literature currently no DPC bound algorithm is readily available to treat also the space frequency power loading problem at the same time.

A simplified frame structure is used such that one instance of the simulation method is run per drop of the channel. A drop represents one statistical realization of a scenario. The Doppler effect is thus not analyzed.

When a system with SDMA and multiple transmitters is considered, a scheduler is needed to assign the users to the transmitters. Since the focus of this work is not on the development of a scheduling algorithm for relay enhanced systems (such as the one in [10] for multiple cells), a genie-like scheduler is used as described below.

The simulation steps for each time slot are as follows:

1. Compute the DPC bound rates for all users when served by each one of the BSs and RNs separately. In the odd time slots RNs do not transmit but are also users (receivers).
2. Genie-like scheduler: Decide on the assignment of users to RNs and BSs based on the achievable DPC rates

from step 1 (no interference considered in this step, suboptimal);

3. Recompute DPC covariance matrices for the newly assigned groups (second run of DPC algorithm required);
4. Perform uplink-downlink conversion of the newly computed covariance matrices as in [11];
5. Compute downlink rates for the entire system WITH interference (all transmitters) using the downlink DPC covariance matrices from step 4 (RN do not transmit and receive in the same time slot);
6. RNs have a buffer: They can only transmit as much data as they have received before (see also below for implementation notes). Limit the achievable rates of the UTs assigned to RNs (from step 6) by the user specific buffer level of the serving RN and sum them up. Fill up the relay buffers in the odd time slots.

Each RN's buffer is implemented as one number rather than storing a vector for each user. The unit of this number is the same as for all rate figures in the procedure, namely  $\text{bits/sec/Hz/m}^2$ . This is the case because no exact time reference is needed for this study, since relative performance is of interest rather than absolute values, and because the TDD slots have equal duration in the present system model.

To generate the buffer levels for each UT needed for step 6 we proceed as follows: When an RN is scheduled for reception, its currently achievable rate is added to its buffer. When an RN is scheduled for transmission, it is assumed that the buffer for transmission to each UT has been loaded optimally based on the achievable rates of the attached users in the current time slot (since we target maximum sum rate rather than user specific quality of service constraints). In real systems, this knowledge is of course not available a priori and represents a simplification which is justified because the channel changes only gradually. In other words, the situation in the time slot in which the buffers would have been filled can be assumed to be similar to the situation when transmission takes place. To generate the user specific buffer levels out of the single value buffer of an RN, the RN buffer figure is distributed via a standard water pouring algorithm on the UTs. To do so, the UTs' achievable rates from step 5 represent the squared coefficients of the channels to be loaded and the RN buffer number is the power to be distributed.

## 4. SIMULATION RESULTS

The IST-WINNER II channel model is used in this investigation. The model and system parameters parameters are kept close to the WINNER baseline system described in [8], except for the restrictions made above on the system model. The parameters relevant to this investigation are described in Table 1. Note that due to limitations in the presently available reference implementation of the channel model, the scenario B5c could not be used for BS to RN and RN to RN connections as suggested in [8]. Instead, B1 is used (which is suggested for the BS to UT links), since it is based on similar parameters.

WINNER model scenario	scenario B1 (as substitute for B5c, see text) (channel model description see [1])
Manhattan grid implementation	building block size $200 \times 200$ m, street width 30 m UT distribution: uniform with density $10^{-5}/\text{m}^2$ random headings and speeds up to 50 km/h BS, RN height 10 m, UT height 1.5 m
Antenna element patterns ( $\lambda/2$ spaced uniform linear arrays with cross polarized antennas)	BS azimuthal: $A(\theta) = -\min\left[12\left(\frac{\theta}{\theta_{3\text{dB}}}\right)^2, 20\right]$ [dB], $\theta_{3\text{dB}} = 70^\circ$ UT azimuthal: $A(\theta) = 1$ elevation gain pattern not supported by the model at present
Receiver noise	thermal noise power spectral density $-174$ dBm/Hz receiver noise figure at RNs 5 dB, at UTs 7 dB
OFDM frequency parameters	frequency reuse 1 (TDD mode) center frequency 3.95 GHz, subcarrier spacing 48828.125 Hz 1664 subcarriers (divided into 104 chunks with same data flow) one subcarrier only simulated due to limitations of DPC bound algorithms
BS transmit power	24 dBm/1664 subcarriers (peak power per BS site)

**Table 1.** Channel modeling and system parameters relevant to this investigation, partially based on [8]

Both terminals and transmitting stations use cross polarized antennas with a directional pattern in azimuth (Table 1). The antennas are placed in ULAs, since this is the antenna geometry currently supported by the reference implementation of the model (see also the deployment descriptions in Section 2).

The case with 8 transmit antennas is shown in Figure 4. Note that the offset of some curves at the probability one point stems from the limited number of points simulated. It can be seen that the overall performance difference of the three deployments is in line with their costs: The most expensive 1D deployment offers the highest performance. However, this is only partially due to the increased BS density. Another reason is that in the cases with higher performance more antennas point into the same direction.

Surprisingly, an increased RN transmit power has only marginal influence. One reason could be that the grid density is still high even at the lowest power setting and that bigger distances and lower power settings should be considered. The 2D strategy is an exception to this observation. It reaches almost the same performance level as displayed by the curves of the 1D strategy when the RN power is at the smallest setting. This supports the observation of the interference limitation.

In the 4 antenna case (Figure 5) we expect a lower array gain and beamforming gain. For example, in the case of the 4D deployment, only one directional antenna is pointing towards each street. As a result, the difference between the deployment strategies is observed to be less than in the 8 antenna case, which suggests that the cheapest deployment strategy could be used when the number of antennas is limited.

Strikingly, when comparing 4 and 8 antennas it can be seen that the range of values is the same and that the deployments with less antennas seemed to be able to provide even a slightly higher overall probability for high rates. When comparing these two cases one must, however, note that the max-

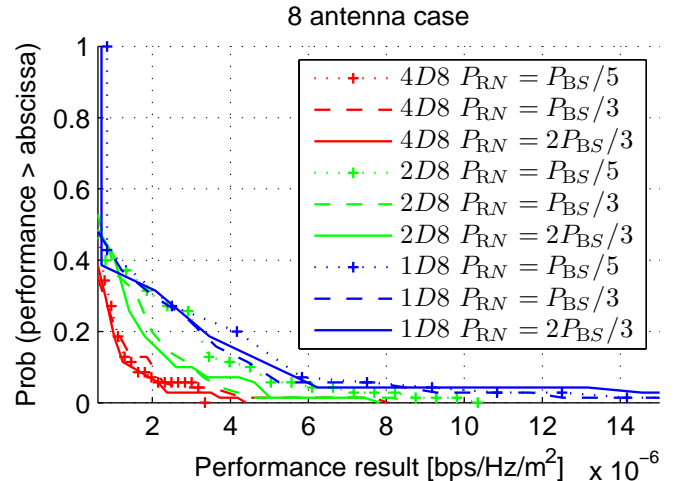


**Fig. 4.** Comparison for the case with 8 antennas

imum sum rate solutions found by the DPC algorithms are not the same in the two different cases and that, therefore, the difference between the two cases is not only in the number of antennas. One reason for this result is that with more antennas the DPC SDMA algorithm tends to serve more users at the same time resulting in smaller fractions of power per user leading to smaller individual rates and leading to a more wide spread total interference in the system. Again, this may indicate that interference avoidance is crucial to exploit the benefits of having more antennas at the transmitters.

## 5. CONCLUSION

It was observed that deployment strategies with higher cost also provide higher total performance. Careful planning of MIMO antenna array directions (and thus coverage direction) is required to exploit those gains in a Manhattan grid sce-

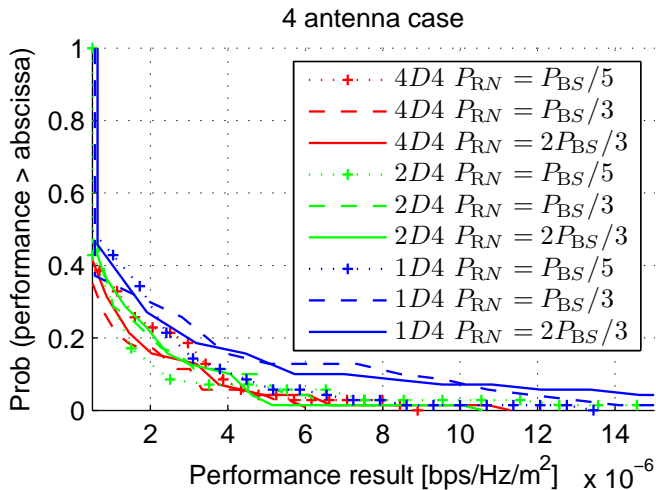


Fig. 5. Comparison for the case with 4 antennas

nario. The use of directional antennas results in an inability to contribute to the beam forming weights with those array elements facing into other streets than the one the receiver is in. Alternative antenna array geometries such as uniform circular arrays should thus be subject of future investigations as well as bigger distances and higher frequency re-use to allow for interference planning. Interference avoidance scheduling seems to be of importance, even in a frequency re-use one setting, as indicated by the fact that an increase in transmit power did not reflect itself in an increase in performance.

## 6. REFERENCES

- [1] "IST-4-027756 WINNER II D1.1: WINNER II interim channel models," November 2006.
- [2] "IST-4-027756 WINNER II D3.5.1: Relaying concepts and supporting actions in the context of CGs," October 2006.
- [3] M. Herdin and T. Unger, "Performance of single and multi-antenna amplify-and-forward relays in a Manhattan street grid scenario," in *IST Mobile and Wireless Communications Summit*, Mykonos, Greece, June 2006.
- [4] B. Wang, J. Zhang, and A. Host-Madsen, "On the capacity of MIMO relay channels," *IEEE Transactions on Information Theory*, vol. 51, pp. 29–43, January 2005.
- [5] C. Lo, S. Vishwanath, and J. R.W. Heath, "Rate bounds for MIMO relay channels using precoding," in *Global Telecommunications Conference, 2005. IEEE GLOBECOM '05*, Dec. 2005.
- [6] H. Bolcskei, R. Nabar, O. Oyman, and A. Paulraj, "Capacity scaling laws in MIMO relay networks," *IEEE Transactions on Wireless Communications*, vol. 5, pp. 1433 – 1444, June 2006.
- [7] "IST-4-027756 WINNER II: D3.4.1 The WINNER II Air Interface: Refined Spatial-Temporal Processing Solutions," November 2006.
- [8] "IST-4-027756 WINNER II D6.13.1: WINNER II Test scenarios and calibration case issue 1," June 2006.
- [9] N. Jindal, W. Rhee, S. Vishwanath, S. Jafar, and A. Goldsmith, "Sum power iterative water-filling for multi-antenna Gaussian broadcast channels," *IEEE Transactions on Information Theory*, vol. 51, pp. 1570–1580, April 2005.
- [10] M. Fuchs, G. Del Galdo, and M. Haardt, "Low complexity spatial scheduling ProSched for MIMO systems with multiple base stations and a central controller," in *Proc. International ITG/IEEE Workshop on Smart Antennas (WSA)*, Guenzburg, Germany, March 2006.
- [11] S. Vishwanath, N. Jindal, and A. Goldsmith, "Duality, achievable rates, and sum-rate capacity of Gaussian MIMO broadcast channels," *IEEE Transactions on Information Theory*, vol. 49, pp. 2658–2668, 10. October 2003.